EPJ Web of Conferences **349**, 01001 (2026) https://doi.org/10.1051/epjconf/202634901001
EMAS 2025

Nanoscale chemical and structural investigation of Mg-doped GaN nanowires using EDS and WDS on SEM

Michael Abratis[1*], *Eric* Robin[2], and *Ralf* Terborg[1]

[1]Bruker Nano GmbH, Am Studio 2D, 12489 Berlin, Germany
[2]Université Grenoble Alpes, CEA, IRIG, 38000 Grenoble, France

Abstract. Semiconductors are the basis of many of today's technical products and therefore an important foundation of our modern economy. One material that is currently the subject of intensive research is doped gallium nitride (GaN), which has outstanding properties, particularly in the form of nanowire structures. For the chemical and structural characterization of such semiconductor nanowires, analyses using EDS and WDS were carried out on a FESEM in this work. The results show that strictly controlled analytical conditions, in particular low primary energy (here 4 keV), are crucial for analysis with high spatial resolution. Only by supplementing the EDS with WDS was it possible to determine both the structure of the nanowires and the trace element content of the dopant Mg (800 ppm). This example proves that advanced analytical questions, in which both high spatial and high spectral resolution are important, can only be solved by using WDS in addition to EDS on SEM.

1 Introduction

1.1 Semiconductor nanowires

Nanowires (NWs) play an important role in modern electronics, storage and conversion of energy, photonics and biomedicine [1-3]. These ultra-thin, wire-like structures with diameters typically in the lower nanometre range and a length of 100s of nanometres to micrometres and beyond can be made from diverse materials such as organics, metals, oxides or semiconductors [4, 5].

Among the semiconductor materials, gallium nitride (GaN) stands out for its superior electrical and thermal properties [3, 6]. Devices based on GaN NWs outperform the traditional Si- based devices due to their higher breakdown strength, faster switching speed, and higher thermal conductivity [7, 8]. Therefore, GaN NWs are increasingly used for optoelectronics, nanoelectronics, sensors, energy devices, metrology tools and quantum devices [5-8]. In order to achieve p-type conductivity for this wide bandgap semiconductor,

* Corresponding author: michael.abratis@bruker.com

© The Authors, published by EDP Sciences. This is an open access article distributed under the terms of the Creative Commons Attribution License 4.0 (https://creativecommons.org/licenses/by/4.0/).

Mg is doped into GaN. This p-type conversion is essential for making devices like LEDs, laser diodes, and high-power transistors [3, 6, 9, 10].

The characterization of elemental doping is crucial for understanding and improving the electrical and optical properties of nanowire semiconductors in order to manufacture reliable and high-performance electronic and optical devices [11, 12]. For detailed characterization of the material and for advanced failure analysis, high resolution imaging and elemental analysis techniques are required. Among them, electron microscopy (SEM, TEM) with electro-optical and spectroscopic techniques are frequently used [11-14].

1.2 X-ray spectroscopy

Two different and complementary X-ray spectroscopy techniques are available for elemental analysis in electron microscopy: EDS (Energy Dispersive X-ray Spectrometry) and WDS (Wavelength Dispersive X-ray Spectrometry).

EDS detects X-rays based on their energy using a semiconductor detector. It is fast and easy to use, however with limited energy resolution, sensitivity and accuracy [15-20].

WDS measures X-rays based on their wavelength using a crystal diffraction system. The technique results in excellent energy resolution, higher sensitivity and accuracy; however, it is slower than EDS (as it scans one wavelength at a time) and it requires standards for quantitative data, what for EDS is not necessarily the case. WDS with PBO (parallel beam optic) is especially advantageous for the low-energy X-rays including the light elements. The superiority of WDS for some analyses is especially obvious when analysing trace elements (< 1 wt.-%) or overlapping peaks [21-25].

Integrated systems with combined EDS and WDS detectors are available for many SEM and provided by different vendors [26-29]. With these set-ups it is possible to combine the best of both worlds: EDS is recommended for rapid, broad-spectrum scans to identify which elements are present. Then WDS is used for detailed checks and for precise quantification of selected elements, especially those in low concentrations or with overlapping peaks. This hybrid approach allows for speed without sacrificing accuracy, and confidence without wasting time [30].

2 Sample and methods

The Mg-doped GaN NWs of the present study are typically up to 1 µm long and 200 nm in diameter. They show axial segmentation with GaN on top, $Al_xGa_{1-x}N$ in the second section, and a base of $In_xGa_{1-x}N$. The NWs were grown by molecular beam epitaxy (MBE) on a substrate of Si (111). During the production of the NWs, care is taken to ensure that their tips are flat and horizontal.

Microanalyses were performed by using a Zeiss Ultra 55 FESEM (Field Emission Scanning Electron Microscope), equipped with a QUANTAX EDS (Energy Dispersive X-ray Spectrometer) and a QUANTAX WDS (Wavelength Dispersive X-ray Spectrometer) for elemental analysis. The applied EDS has a silicon drift detector (SDD) of 30 mm² active area and 127 eV resolution (@Mn Kα) and a super light element window. The WDS is equipped with a grazing incidence parallel beam X-ray optic (PBO) and 6 diffraction crystals.

The SEM was operated with a primary energy of 10 keV and 4 keV, respectively, and a beam current of 5 nA in both cases. The analyses were first performed at higher keV values to achieve a maximum pulse rate for good statistics and then gradually reduced until we could ensure that only the top layer was affected by the excitation volume (checking for indicator elements of the underlying layers). Simultaneous acquisitions and combined EDS-WDS quantification was done using the ESPRIT software.

EDS measurements were done with low dead times, long peak shaping times and ca. 5 x 10^6 counts per spectrum. All quantifications were performed standards-based using certified reference material (GaN, MgO).

For WDS, the TAP crystal was used for energy range scans between 0.9 and 1.6 keV, and an 80 Å multilayer for scans from 0.35 to 0.45 keV. Certified reference material (synthetic MgO and GaN) was used for standard-based quantification. For quantitative trace element analyses by WDS, the counting time was set to 300 s for peaks and 150 s for backgrounds. Ga was measured with a 30 s counting time on peak and N with a 60 s counting time. A linear interpolation was applied between the background positions below and above the element peaks to determine the net counts. Matrix correction was done using the $\phi(\rho z)$ method of XPP [31] for both, EDS and WDS. The analytical uncertainty was calculated based on the respective net counts but also includes uncertainties related to the noise statistics and the atomic data (e.g. MACs).

3 Results and discussion

3.1 Chemical segmentation

The sample investigated in this study consists of NWs with characteristically high aspect ratios (ca. 1 µm length and 200 nm diameter). The structures to be resolved are in the hundreds to tens of nanometre range and therefore require very high spatial resolution for the analysis.

Prior to the analysis, it was already known that the NWs have an axially segmented structure, although the respective thickness of these layers was unclear. The stem of the NWs consists of indium gallium nitride ($In_xGa_{1-x}N$), the central layer is made of aluminium gallium nitride ($Al_xGa_{1-x}N$), while the top layer of Mg-doped gallium nitride (GaN:Mg). A SE image and a schematic representation of the sample structure is shown in Figure 1.

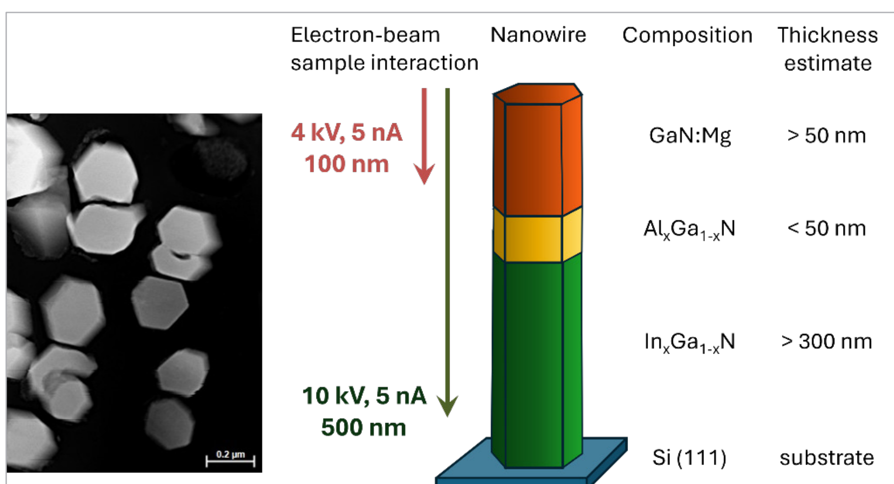

Fig. 1. SE image of the GaN-NWs in top view and a schematic drawing showing the chemical layering of the NWs together with the electron-beam – sample interaction depth as derived from modelling and analytical results.

The aim of our study was to accurately determine the concentration of the trace element Mg in the doped GaN layer of the NWs. This requirement clearly means that the depth of the

analysis had to be limited to the top layer of the NWs, also because the limitation to a homogeneous sample volume is crucial for any X-ray based quantification.

3.2 Electron-beam – sample interactions

The excitation volume generated by an electron beam in any sample depends on the composition of the sample and on the primary beam energy. These relationships have been known since the work of Anderson & Hasler (1966) [32] and can be modelled using Monte Carlo simulations such as those derived by Casino [33].
The results of such modelling for 10 and 4 keV primary energy for the given sample composition are shown in Figure 2. Applying a primary energy of 10 keV leads to an X-ray excitation depth of up to 500 nm in the present material, as suggested by the modelling results (Fig. 2). When the primary energy is reduced to 4 keV, the X-ray excitation depth is limited to only 100 nm.

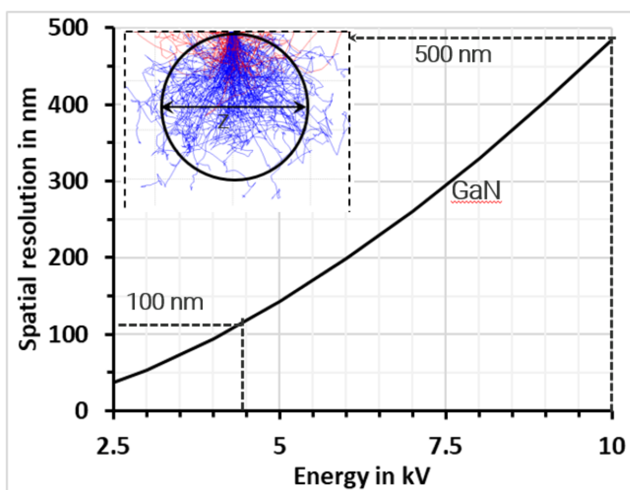

Fig. 2. Modelling of the electron - sample interaction at 10 keV and 4 keV and resulting excitation depths. The freeware Casino 2.42 was used for modelling [33].

Moreover, also the beam diameter is of interest for the spatial resolution of the analysis. The narrow, high-brightness beam of a FESEM (Field Emission Scanning Electron Microscope) not only enables high-resolution imaging but may also restrict the excitation volume for high-density samples investigated at low keV.

The small diameter of the individual NWs clearly imposes an analytical challenge and limits the accuracy of quantification which assumes lateral infinite size. Applying a primary energy of 10 keV generates an excitation volume whose lateral extent (cf. Fig. 2) significantly exceeds the diameter of a single NW. Electron – sample interaction modelling at 4 keV and 5 nA however indicates an excitation width of only ca. 100 nm diameter (cf. Fig. 2) that is consistent with the diameter of a single NW (ca. 200 nm).

3.3 EDS and WDS parameters

Previous work on determining the Mg content in gallium nitride using EDS has already highlighted the analytical challenges resulting from the strong peak overlap of Mg Kα with

the Ga L line series [13, 14]. Not only are the line positions very close to each other (Δ eV Mg Kα – Ga Lβ3 = 55 eV), but the peak intensities are also extremely different, as one of the elements is a major element and the other a trace element. Any deconvolution attempts are thus facing their limits. Furthermore, a strong peak overlap for In Mζ with N Kα (Δ eV = 26 eV) makes the discrimination of these two elements unfeasible for EDS at low keV.

High spectral resolution and sensitivity is therefore crucial for the given analytical task and can be provided by a PBO-WDS on the SEM, which has high performance for the low-energy X-ray lines.

In order to test the suitability of the WDS for solving the analytical problem, we determined the spectral resolution and the detection limits under the relevant analytical conditions. The measurement results derived from standard materials at 10 keV and 5 nA are presented in Figure 3. The spectral resolution of the PBO-WDS determined as FWHM (full width at half peak maximum) is 4-20 times better than that of the EDS. The limits of detection (calculation adapted from Love and Scott, 1983 [34]) derived from the signal-to-noise ratio are up to 10 times better than those of the EDS under the given analytical conditions.

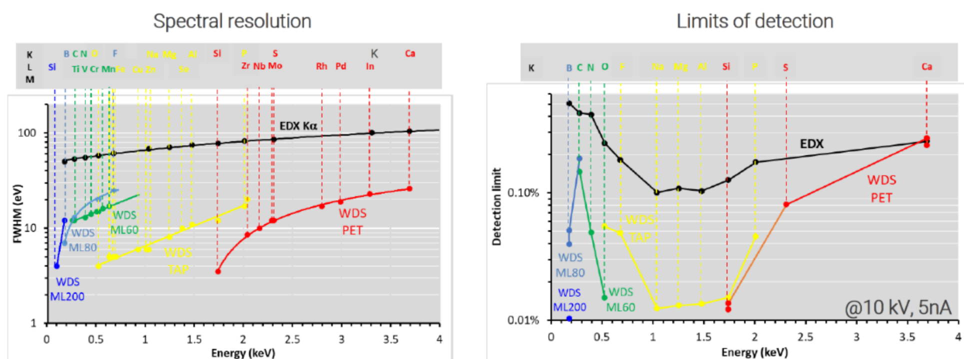

Fig. 3. EDS and WDS spectral resolution described as Full Width at Half peak Maximum (FWHM) and limit of detection at 10 keV, 5 nA.

3.4 Spectroscopic results

Spectroscopic analyses in the SEM were done in NW axial direction (view from top) and first using 10 keV primary energy.

Both techniques (EDS and WDS) document the presence of Ga and N peaks, but with different accuracy: WDS energy range scans resolve the different Ga L lines and even identifies a small peak for Mg Kα.

In addition to the main peaks for Ga and N, the EDS spectrum shows a peak for Al, which was also confirmed by WDS energy range scans (Fig. 4). The presence of Al in the spectra proves that the second layer of the NWs was probed at the present conditions using 10 keV.

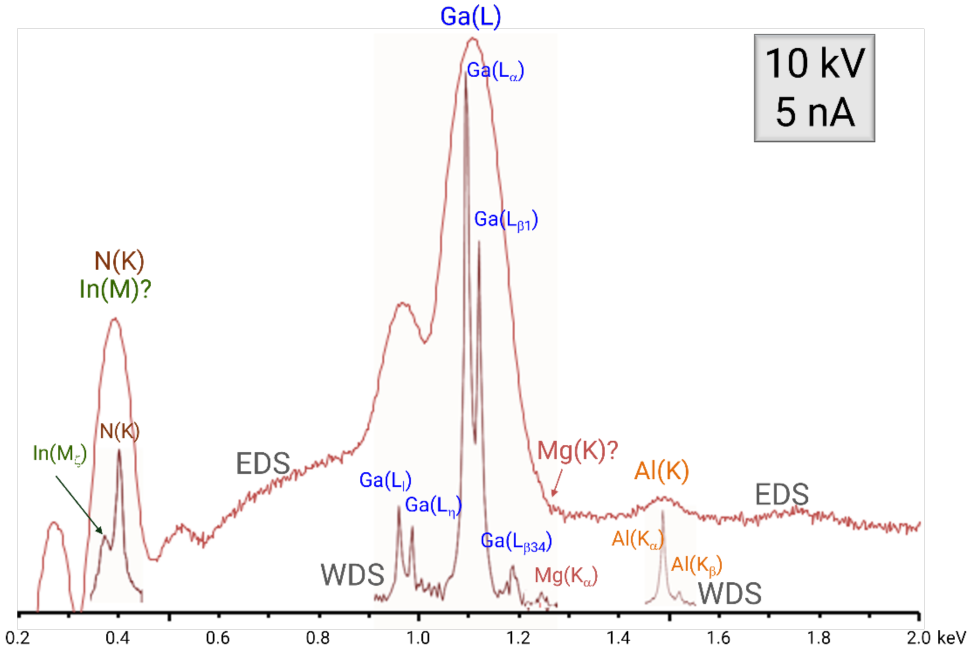

Fig. 4. EDS and WDS spectra acquired at 10 keV. In contrast to EDS, WDS can resolve the overlaps and reveal the presence of In and Mg in the analysed volume.

A WDS energy range scan at low X-ray energies shows the presence of a peak of In Mζ at 366 eV, proving that the indium-containing base layer of the NWs was also excited at 10 keV primary energy. Due to the strong overlaps between N (K) and In (M-lines) as well as Mg (Kα) and Ga (L-lines), the EDS spectrum could not provide any information about possible proportions of In and Mg in the analysis.

Based on these findings and in order to limit the excitation volume only to the NW top layer (GaN:Mg), the primary energy was reduced to 4 keV. The corresponding modelling of the electron-sample interaction (Fig. 2) shows that at 4 keV the X-ray excitation depth is limited to approx. 100 nm.

The results of the EDS and WDS analysis at 4 keV are shown in Figure 5. The absence of In and Al in the spectra indicates that the excitation volume is limited to the top layer. From this it can be concluded that the active NW layer (GaN:Mg top layer) is at least 100 nm thick. By gradually increasing the primary energy until the X-ray lines for In and Al reappear in the spectra, the structure and the respective layer thickness of the NWs can be deciphered.

Since the spectral data show that the excitation volume at 4 keV is limited to the NW top layer, the Mg doping concentration in GaN can be reliably determined. While any small peak for Mg Kα would not be visible for EDS since it completely disappears in the tail of the prominent peak for Ga L, the WDS clearly resolves these peaks. Using peak/background measurements and standards-based quantification, the Mg concentration in the NW top layer was determined to be 0.08 ± 0.01 wt.-% (average value and standard deviation for the analysis of 5 individual NWs).

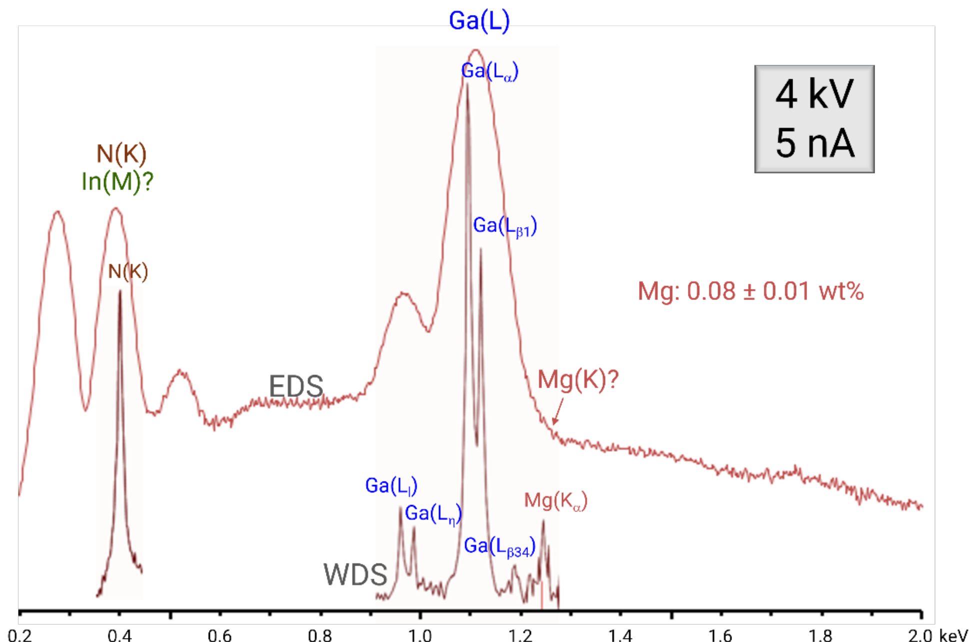

Fig. 5. EDS and WDS spectra simultaneously acquired at 4 keV. Due to strong overlaps, EDS cannot provide any indication of the presence or absence of In and Mg. However, the WDS spectrum clearly shows the absence of a peak for In and a significant peak for Mg Kα. The content of the Mg dopant can be determined by WDS at 800 ppm.

4 Conclusion

The accurate analysis of trace elements in small samples such as the NWs requires both a high spatial and a high spectral resolution. First, the limited size restricts the analytical conditions, which leads to considerable analytical challenges: To achieve high spatial resolution, low-keV must be used. The use of low-keV in turn limits the generated X-ray spectrum to low energies, a range in which the EDS shows particularly large overlaps. EDS microanalysis proved to be insufficient for the requested quantification of trace element contents of Mg in GaN. Only WDS microanalysis, especially with a modern parallel-beam WDS being highly sensitive for the low-energy part of the spectrum and showing better energy resolution and trace element performance can provide a remedy here. Mg- and Ga-peaks could well be resolved by WDS, allowing the quantification of 800 ppm Mg in the active GaN layer. Besides the trace element quantification, also the structure of the NWs could be elucidated: From the qualitative element findings by WDS at different keVs in conjunction with the respective modelling results for beam – sample interaction we can conclude that the total length of the NWs (including GaN:Mg top layer, $Al_xGa_{1-x}N$ intermediate layer and $In_xGa_{1-x}N$ base layer) exceeds 500 nm, while the top layer has a thickness in between 100 nm and < 500 nm.

This example on the investigation of NWs documents how important it can be for certain applications to extend the range of available microanalysis tools with a parallel beam WDS to enable analysis beyond the limitations of EDS. The combined analysis by EDS and WDS on SEM allows the exact determination of the NW composition including major and trace elements as well as the identification of chemical heterogeneities, offering valuable information for enhancing device design and material processing approaches.

The data supporting the results of this study are available on request from the corresponding authors.

The authors would like to thank the reviewers for their constructive comments, which have contributed to the improvement of the manuscript.

References

1. C.M. Lieber, Nanoscale Science and Technology: Building a Big Future from Small Things. MRS Bulletin **28**, 486–491 (2003). https://doi.org/10.1557/mrs2003.144
2. Y. Cui, X. Duan, Y. Huang, C.M. Lieber, Nanowires as Building Blocks for Nanoscale Science and Technology. In Z.L. Wang (ed) Nanowires and Nanobelts (Springer, Boston, MA, 2003). https://doi.org/10.1007/978-0-387-28745-4_1
3. Y. Li, F. Qian, J. Xiang, C.M. Lieber, Nanowire electronic and optoelectronic devices, Materials Today **9**, 18-27 (2006). https://doi.org/10.1016/S1369-7021(06)71650-9
4. Y. Huang, C.M. Lieber, Integrated nanoscale electronics and optoelectronics: Exploring nanoscale science and technology through semiconductor nanowires. Pure and Applied Chemistry **76**, 2051-2068 (2004). https://doi.org/10.1351/pac200476122051
5. M.S. Dresselhaus, M.R. Black, V. Meunier, O. Rabin, Nanowires. In B. Bhushan (ed) Springer Handbook of Nanotechnology (Springer, Berlin, Heidelberg, 2017). https://doi.org/10.1007/978-3-662-54357-3_9
6. M. Shur, Wide band gap semiconductor technology: state-of-the-art, Solid State Electron. **155**, 65-75 (2019). https://doi.org/10.1016/j.sse.2019.03.020
7. E.A. Jones, F.F. Wang, D. Costinett, Review of commercial GaN power devices and GaN-based converter design challenges, IEEE, J. Emerg. Sel. Top. Power Electron. **4**, 707-719 (2016). https://doi.org/10.1109/JESTPE.2016.2582685
8. Y. Zhong, J. Zhang, S. Wu, L. Jia, X. Yang, Y. Liu, Q. Sun, A review on the GaN-on-Si power electronic devices, Fundam. Res. **2**, 462-475 (2022). https://doi.org/10.1016/j.fmre.2021.11.028
9. R. Vermeersch, E. Robin, G. Jacopin, B. Gayral, J. Pernot, B. Daudin, Comprehensive Electro-Optical Investigation of a Ga-Doped AlN Nanowire LED for Applications in the UV-C Range. ACS Appl. Nano Mater. **6**, 13945-13951 (2023). https://doi.org/10.1021/acsanm.3c01705
10. E. Akar, I. Dimkou, A. Ajay, E. Robin, M.I. den Hertog, E. Monroy, GaN and AlGaN/AlN Nanowire Ensembles for Ultraviolet Photodetectors: Effects of Planarization with Hydrogen Silsesquioxane and Nanowire Architecture, ACS Appl. Nano Mater. **6**, 12792–12804 (2023). https://doi.org/10.1021/acsanm.3c01496
11. J. Kamimura, P. Bogdanoff, M. Ramsteiner, P. Corfdir, F. Feix, L. Geelhaar, H. Riechert, p-Type Doping of GaN Nanowires Characterized by Photoelectrochemical Measurements, Nano Lett. **17**, 1529 (2017). https://doi.org/10.1021/acs.nanolett.6b04560
12. E. Aybeke, A.-M. Siladie, R. Vermeersch, E. Robin, O. Synhaivskyi, B. Gayral, J. Pernot, B. Daudin, G. Bremond, Nanoscale imaging of dopant incorporation in n-type and p-type GaN nanowires by scanning spreading resistance microscopy, J. Appl. Phys. **131**, 075701 (2022). https://doi.org/10.1063/5.0080713
13. E. Robin, N. Mollard, K. Guilloy, N. Pauc, P. Gentile, Z. Fang, B. Daudin, L. Amichi, P.-H. Jouneau, C. Bougerol, M. Delalande, A.-L. Bavencove, Quantification of

Dopants in Nanomaterial by SEM/EDS. In Proceedings of the European Microscopy Congress 2016, European Microscopy Society, Wiley-VCH, Weinheim, Germany (2016), 380–381 https://doi.org/10.1002/9783527808465.EMC2016.6335

14. A.-M. Siladie, L. Amichi, N. Mollard, I. Mouton, B. Bonef, C. Bougerol, A. Grenier, E. Robin, P.-H. Jouneau, N. Garro, A. Cros, B. Daudin, Dopant radial inhomogeneity in Mg-doped GaN nanowires, Nanotechnology **29**, 255706 (2018). https://iopscience.iop.org/article/10.1088/1361-6528/aabbd6
15. J.I. Goldstein, D.E. Newbury, J.R. Michael, N.W.M. Ritchie, J.H.J. Scott, D.C. Joy, Scanning electron microscopy and X-ray microanalysis. 4th ed. (Springer, New York, 2017). https://doi.org/10.1007/978-1-4939-6676-9
16. J. J. Friel, R. Terborg, S. Langner, T. Salge, M. Rohde, J., X-Ray and Image Analysis in Electron Microscopy, (Berlin, Bruker Nano GmbH, 2017) ISBN 978-3-86460-674-8
17. R. Terborg, M. Rohde, New developments in state of the art silicon drift detectors (SDD) and multiple element SDD. In M. Luysberg, K. Tillmann, T. Weirich (eds) EMC 2008 14th European Microscopy Congress 1–5 September 2008, Aachen, Germany. (Springer, Berlin, Heidelberg, 2008). https://doi.org/10.1007/978-3-540-85156-1_317
18. D.E. Newbury, N.W.M. Ritchie, Performing elemental microanalysis with high accuracy and high precision by scanning electron microscopy/silicon drift detector energy-dispersive X-ray spectrometry (SEM/SDD-EDS). Journal of Material Science **50**, 493–518 (2015). https://doi.org/10.1007/s10853-014-8685-2
19. R. Terborg, T. Salge, P. Pinard, S. Richter, Deconvolution of EDS steel spectra using low acceleration voltages and low energy X-ray lines. In Proceedings of the European Microscopy Congress 2016, Weinheim, Germany, Wiley-VCH Verlag (2016), 762-763. https://doi.org/10.1002/9783527808465.EMC2016.6519
20. D.E. Newbury, N.W.M. Ritchie, Electron-excited X-ray microanalysis by energy dispersive spectrometry at 50: analytical accuracy, precision, trace sensitivity and quantitative compositional mapping. Microscopy and Microanalysis **25**, 1075–1105 (2019). https://doi.org/10.1017/S143192761901482X
21. S.J.B. Reed, Electron Microprobe Analysis, (Cambridge Univ. Press, Cambridge, 1993) ISBN 0-521-41956-5
22. S.J.B. Reed, Electron microprobe analysis and scanning electron microscopy in geology, 2nd ed. (Cambridge University Press, Cambridge, 2010). https://doi.org/10.1017/CBO9780511610561
23. R. Rinaldi, X. Llovet, Electron Probe Microanalysis: A Review of the Past, Present, and Future, Microscopy and Microanalysis **21**, 1053–1069 (2015) https://doi.org/10.1017/S1431927615000409
24. J.M. Allaz, M.L. Williams, M.J. Jercinovic, K. Goemann, J. Donovan, Multipoint background analysis: Gaining precision and accuracy in microprobe trace element analysis. Microscopy and Microanalysis **25**, 30-46 (2019). https://doi.org/10.1017/S1431927618015660
25. X. Llovet, A. Moy, P.T. Pinard, J.H. Fournelle, Reprint of: Electron probe microanalysis: A review of recent developments and applications in materials science and engineering, Progress in Materials Science **120**, 100818 (2021) https://doi.org/10.1016/j.pmatsci.2021.100818
26. Bruker Electron Microscope Analyzers, QUANTAX WDS, Wavelength Dispersive Spectrometry for SEM, https://www.bruker.com/en/products-and-solutions/elemental-analyzers/eds-wds-ebsd-SEM-Micro-XRF/quantax-wds.html

27. Gatan Ametec EDAX Lambda WDS Spectrometers https://www.edax.com/products/wds/lambda-wds-analysis-system
28. Oxford Instruments, Wavelength Dispersive Spectroscopy (WDS) https://nano.oxinst.com/products/wds/
29. Thermo Scientific WDS MagnaRay Spectrometer https://www.thermofisher.com/order/catalog/product/de/en/IQLAADGABJFAKQMAVG
30. L. Maniguet, F. Robaut, A. Meuris, F. Roussel-Dherbey and F. Chariot, X-ray microanalysis: the state of the art of SDD detectors and WDS systems on scanning electron microscopes (SEM), IOP Conf. Ser.: Mater. Sci. Eng. **32**, 012015 (2012). https://iopscience.iop.org/article/10.1088/1757-899X/32/1/012015
31. J.L. Pouchou, F. Pichoir, Quantitative Analysis of Homogeneous or Stratified Microvolumes Applying the Model “PAP”. In K.F.J. Heinrich, D.E. Newbury (Eds), Electron Probe Quantification, (Plenum Press, New York, 31-75, 1991) https://doi.org/10.1007/978-1-4899-2617-3_4
32. C. A. Anderson, M. F. Hasler, In Proceedings of the 4th International Conference on X-ray Optics and Microanalysis (R. Castaing, P. Deschamps, J. Philibert, eds.), Hermann, Paris (1966), 310
33. D. Drouin, A.R. Couture, D. Joly, X. Tastet, V. Aimez, R. Gauvin, CASINO V2.42 - A Fast and Easy-to-use Modeling Tool for Scanning Electron Microscopy and Microanalysis Users, Scanning, **29**, 92-101 (2007). https://doi.org/10.1002/sca.20000
34. G. Love, V.D. Scott, Calculation of Detection Limits and Analytical Sensitivity in Electron Probe Microanalysis. Unpublished technical note (1983). Referenced in EPMA software documentation. https://documentation.help/EPMA-Probe/calculatedetectionli.htm